

Flexible Electrostatic Transducers for Wearable Haptic Communication*

Ian H. Trase, Zhe Xu, Zi Chen*, Hong Z. Tan*, *Fellow, IEEE*, and John X.J. Zhang*, *Senior Member, IEEE* (* co-corresponding authors)

Abstract— We describe a wearable thin-film flexible electrostatic transducer (FET) design capable of delivering haptic stimulation directly to the skin over a broad frequency range. The FET vibrates a curved electrode on a thin film against the skin to generate perceivable displacement. Performance was characterized and studies were carried out to benchmark the comfort and perceptibility on human subjects. Specifically, we conducted a psychophysical experiment to estimate detection thresholds at low (26Hz) and high (260Hz) frequencies and estimated the maximum level at which the stimuli remained comfortable. The displacement response of the FET was highly nonlinear, actuating close to either zero or maximum displacement after a threshold driving amplitude. The 260Hz vibrations were detected at lower displacements than the 26Hz vibrations. In user studies, the detection thresholds indicated that the current FET design achieved a 10dB perceivable stimulation range at both frequencies. No significant difference was found for gender or forearm location. Participants found all low amplitude signals to be comfortable, while at maximum amplitude the low frequency (26Hz) signal was preferred. The present study provides a methodology to quantitatively characterize actuator performance in terms of human perception.

I. INTRODUCTION

Haptic communication transfers information such as speech through the sense of touch. That the sense of touch is capable of high information transmission has been demonstrated by natural tactual communication methods by deaf and deaf-and-blind individuals [1]. Many studies have also demonstrated device-mediated speech communication via the haptic channel [2]–[5]. Device wearability varies, with systems using ERMs (eccentric rotary motors) and LRAs (linear resonant actuators) being more wearable due to small form factors and low power consumption. Broadband actuators such as voice-coils and piezoelectric actuators are more “expressive” in that they are capable of delivering multidimensional, richer sensations that have been shown to increase information transfer [6], [7]. Yet they tend to be less wearable due to their larger size, stiffness, difficulty with mounting, high driving voltage, etc. This may explain

*Research supported by Facebook, Inc. under the SARA program; The Society in Science Branco Weiss Fellowship administered by ETH Zürich; and the NIH Director’s Transformative Research Award (R01HL137157, PI: J.X.J.Z).

Ian Trase, Zhe Xu, Zi Chen, and John X.J. Zhang are with the Thayer School of Engineering at Dartmouth College, Hanover, NH 03755 USA (e-mail: zi.chen@dartmouth.edu; john.zhang@dartmouth.edu).

Hong Z. Tan is with the School of Electrical and Computer Engineering at Purdue University, West Lafayette, IN 47907 USA (e-mail: hongtan@purdue.edu).

why most commercially-available wearables use ERMs and LRAs for haptic notification (see Fig. 1). A growing number of applications such as social touch [8], navigation [9], VR/AR manipulation [10], [11], and silent communication [12], [13] can benefit from haptic actuators that are thin and flexible and can disappear into garments and wearable devices. The research demonstrates a first step towards this goal through a close collaboration between mechanical engineers and hapticians.

We explored the possibility that flexible thin-film electrodes and mechanical buckling could be used to build a transducer with high comfort and perceptibility. Previously, we have developed a series of thin film piezoelectric transducer technologies for biosensing applications [14]–[18]. Here we investigated how electrostatic actuation could be used to build a transducer that took advantage of the skin’s sensitivity to certain modes and frequencies of vibration. The characteristics of flexible electrostatic actuators make them particularly well-suited to haptic applications. Flexible and curved electrodes have been studied previously in the application of micro-electromechanical (MEM) devices, as they do not suffer from electrostatic pull-in [19], [20]. These devices tend to respond rapidly to changes in stimuli, conform comfortably to the skin, and are resilient to environmental and mechanical damage. They are also extremely lightweight, as the fundamental mechanism is simply composed of a pair of

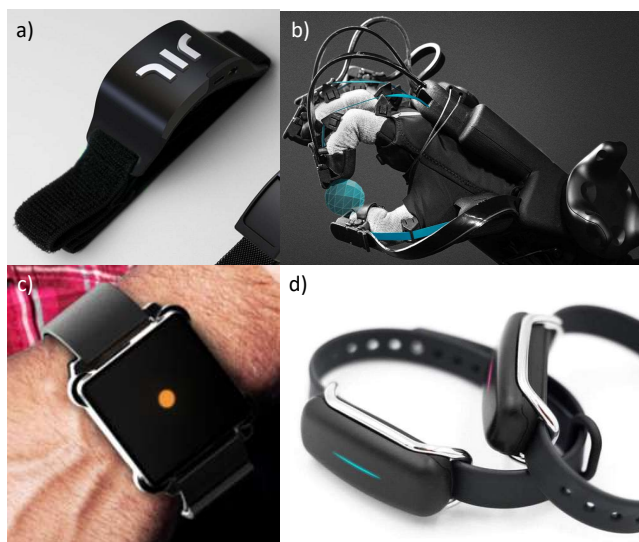


Figure 1: Haptic wearable devices. A) Wayband navigation aid for the blind and visually impaired (<https://www.wear.works/wayband/>). B) HaptX Glove for VR and AR touch (<https://haptx.com/>). C) Moment wearable for touch notifications (<https://somaticlabs.io/>). D) Bond Touch for interpersonal touch-at-a-distance (<https://www.bond-touch.com>)

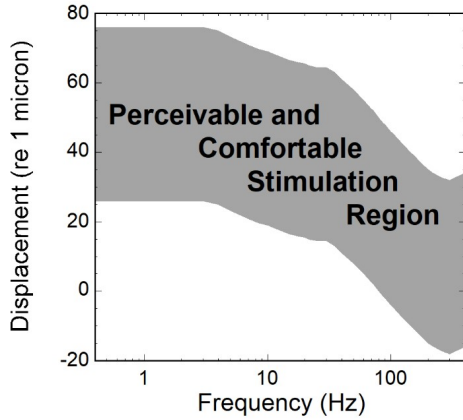


Figure 2: Schematic illustration of “perceivable and comfortable stimulation region” with data from [24].

thin films moving against one another. Other flexible electrostatic transducers have been designed, but they often involve dielectric elastomers, which require extremely high voltages [21], [22]. Even actuators which use similar airgap-inspired approaches have issues with voltage and pull-in instabilities [23].

We designed and built a wearable flexible electrostatic transducer (FET) capable of comfortably delivering vibration directly to the skin. To test this transducer, we conducted a psychophysical experiment to determine the detection thresholds at two distinct frequencies and two forearm locations. There are many ways that the performance of haptic technologies such as the FET can be specified, and most company brochures and published studies use engineering specifications such as the frequency range, peak acceleration, peak displacement, and/or peak force. While such engineering specifications do allow for comparison of different actuators, they do not inform the range of human perception that the actuators are able to stimulate. This is because human sensitivity to skin contact varies significantly with signal frequency by about 48 dB (see Fig. 2). It would be more useful to characterize actuator performance in terms of achievable range of *perceived intensities* as a function of frequency. To visualize this, we show schematically the “perceivable” range of vibrotactile signals, from detection threshold (the smallest perceivable vibration) to 50 dB above that (discomfort threshold), over a frequency range of 0.4-400 Hz based on data from [24] collected on the thenar eminence (the fleshy part at the base of the thumb) (Fig. 2). In psychophysical terms, stimulation intensities are specified in dB sensation level (SL), which is dB above detection thresholds (lower limits of the shaded region). Perceived intensities are roughly equivalent to the sensation levels [25]. We therefore benchmark the FET actuators against the shaded area in Fig. 2. The extent to which the actuators can cover the shaded “Perceivable and Comfortable Stimulation Region” provides a human-centered metric for the performance of the actuators in terms of their usefulness as haptic stimulators. Typically, stimulation is clearly perceivable and comfortable at 10-20 dB SL, and become too strong or uncomfortable above 40 dB SL. As a first step, we measured detection thresholds at

26 and 260 Hz, two frequencies with significantly different detection thresholds according to earlier studies [24].

The present research makes three contributions. First, we developed a new actuator for wearable haptics based on a flexible electrostatic transducer. Second, we characterized the physical operations of the new transducer. Third, we measured the human detection threshold at two distinct frequencies to quantify the perceived-intensity range that can be achieved with the new transducer.

II. THEORY OF OPERATION

We have developed a flexible electrostatic transducer capable of delivering precise vibrations to the skin [26]. The device consists of a pair of thin electrode films separated by an air gap, with one electrode fixed and the other free to move. When a sinusoidal voltage is applied, the free film moves in and out of contact with the fixed film. This generates an easily-perceived vibration when placed on the skin. The transducer itself is lightweight, weighing only 2.2 grams with an included holder. Its flexible design allows it to conform and move with the skin, which improves both force transmission and comfort. Because the method of actuation is purely electrostatic, the transducer responds rapidly to driving signals and can support high frequencies. As a haptic wearable, the transducer’s simple design and few moving parts improve its resilience to mechanical damage and the environment. This combination of lightweight flexibility, speed, and reliability make this transducer well-suited to haptic communication.

A schematic of the transducer operation and an image of the prototype device are shown in Fig. 3a and 3c. The transducer consists of a 20x20 mm piece of 25 μ m thick Kapton film sputter-coated with 20nm of gold electrode and fixed to a rigid 3D-printed plastic holder. A second 21mm by 20mm electroded Kapton film is then attached to the first film, with both electrodes facing towards the rigid surface. Because the second film is slightly longer than the first, it

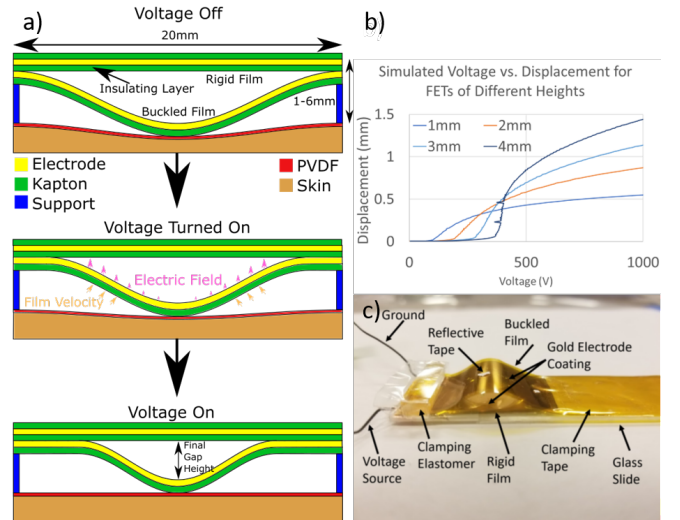


Figure 3: Flexible electrostatic transducer (FET). A) schematic of operation. Initially buckled film is pressed into the skin. Applied voltage pulls the film away from the skin, and voltage release cause the film to depress again. B) Simulated voltage-displacement curves for a FET with heights from 1mm to 4mm. C) Annotated photograph of the finished device on a glass slide for direct laser vibrometer measurement showing the various components.

buckles into a cosine-shape when adhered. A wire is attached to each electrode using adhesive copper tape. This pair of wires is connected to a Trek model 2210 high voltage supply capable of supplying a maximum amplitude of 1000V and a gain of 100V/V, which is isolated through a Triad Magnetics MD-250-E medical-grade isolation transformer. A voltage signal is generated from the 3.5mm audio jack of a desktop PC with a maximum output amplitude of $\sim 2V$. This signal is amplified by a simple op-amp circuit to have a maximum amplitude of $\sim 10V$ and then delivered to the high voltage amplifier.

When a voltage is applied between the two electrodes, electrostatic attraction pulls the two films into contact. The extent of this contact and the equilibrium shape of the transducer at a given voltage is the result of a competition between bending and electrostatic energy. As the buckled film is pulled closer to the fixed film, the electrostatic force increases, pulling the film further in. This positive feedback loop is known as electrostatic pull-in and is often a problem in micro-electromechanical devices (MEMS). This pull-in is resisted as the flexible buckled film bends. As the curvature of the buckled film increases, a restorative bending force begins to increase faster than the electrostatic force and eventually brings that device into a static equilibrium. This energy balance can be approximated by Equation 1:

$$\frac{1}{2} \epsilon_K \frac{V^2}{\int h^2(s) ds} - \frac{1}{2} \int \sigma(s) S(s) ds = 0 \quad (1)$$

Here ϵ_K is the permittivity of Kapton, V is the instantaneous voltage between the two films, s is the arc-length location along the buckled film, $h(s)$ is the vertical distance between the two electrodes, $\sigma(x)$ is the stress tensor of the buckled film, and $S(s)$ is the strain tensor of the buckled film.

At low voltages, the electrostatic force between the two films is low, and there is no motion. At a critical voltage, the electrostatic force is high enough to move the buckled film into contact with the fixed film, and the film will rapidly compress until the electrostatic force is balanced by the restoring force of the film. This relationship between voltage and displacement is shown in the 26Hz plot in Fig. 4a. The transducer has three characteristic regions. In the first region, motion of the free film is not triggered because the applied voltage is low. Next, when the voltage is close to the critical value, the free film is attracted toward the fixed one and its displacement rises rapidly with voltage. In the final stage, the free film generates a large bending-based restoring force and the displacement is near-constant, with exponentially higher voltages required to drive linear increases in displacement. This relationship is confirmed by laboratory tests in which the transducer is free to move. When the transducer is attached to a mechanical load, the second stage in which displacement rises rapidly with voltage is muted and stretched out. This results in higher voltages being necessary to reach the same displacement. The geometry of the transducer also has a large effect on the voltage-displacement curve. In general, transducers with larger air gaps require higher voltages to begin actuation but can reach greater displacements and output larger force. The thickness of the fixed film directly controls the electric field strength between

the electrodes, and a thinner fixed film will result in voltages that are significantly lower.

We conducted finite element simulations to verify the response of the transducer and to characterize the voltage-displacement response. A 2D model was designed in COMSOL using tetragonal elements for the buckled film and rectangular mapped elements for the air gap between the films. The center of the buckled film was assigned a fixed displacement, and the voltage needed to achieve this displacement was then calculated. This procedure was then repeated with increasing prescribed displacements until the buckled film had become completely flush with the rigid film or until the buckled film self-intersected. To increase accuracy and decrease computation time, the solution to the previous displacement level was used as the initial condition for the next level. Simulations were conducted for four different device geometries of increasing height, from 1mm to 4mm in differences of 1mm. The rigid film was not modeled, and instead a custom-designed contact boundary was put in place to accurately model the shape of the buckled film as it flattened against the rigid film.

The simulations, shown in Fig. 3b, show the basic response of the transducer in air. When the gap between the center of the buckled film is small, at 1mm, the threshold voltage needed to begin transducer actuation is lower, as is the ultimate displacement. The initial rate of change in voltage as the displacement increases is also lowest for this geometry. As the transducer becomes taller, the threshold voltage to begin actuation and the maximum displacement at 1000V also rise. In addition, we see an increase in the rate of change in voltage as displacement increases. For very tall simulated transducers (>6), we observed a snap-through effect, where the required voltage to statically maintain the shape decreases as the displacement increases. These simulations elucidate the fundamental tradeoff between device height and required voltage and allow us to rationally design a transducer with an acceptable displacement and voltage requirement.

Because the FET is flexible, it can conform to the skin and make correct contact no matter where it is placed. The motion of the buckled film during operation results in repeatedly making and breaking contact with the skin, which

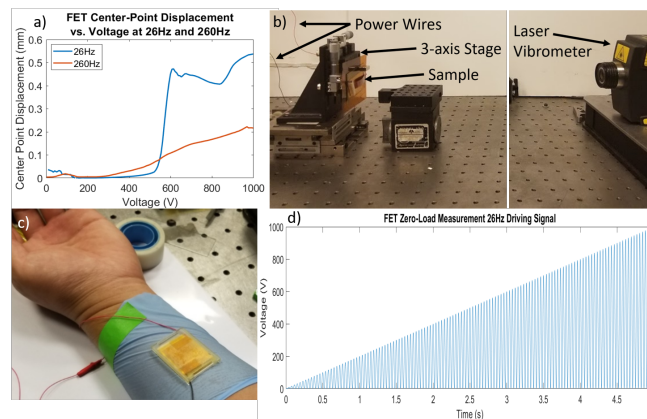


Figure 4: Zero-load displacement of FET. A) Plot of displacement vs. voltage from 0-1000V for a 26Hz and 260Hz driving signal. B) Photographs of laser vibrometer measurement setup for FET. C) Photograph of FET on volar side of forearm. D) Driving signal for FET testing. Signal ramps from 0 to 1000V peak-to-peak at 26Hz while remaining positive.

has been shown to increase perception over sustained changes in pressure [27]. We chose 26Hz and 260Hz because they correspond to the two frequency regions at which the Meissner's and Pacinian corpuscles are most sensitive, respectively [24], [25], [28], [29]. The Pacinian corpuscle mechanoreceptors in the skin are most receptive to frequencies between 200-300Hz [28], while the Meissner's corpuscles are sensitive to frequencies from 10-50Hz [29].

III. DEVICE CHARACTERIZATION AND EXPERIMENT

The transducer was tested both under a load free condition and pressed against the skin. Fig. 4b shows a testing setup designed to measure the zero-load displacement of the transducer as a function of voltage. The transducer is mounted vertically to a three-axis stage and connected to the high voltage amplifier and a Keysight 33522B signal generator. A small piece of reflective tape is adhered to the top of the transducer to maximize the reflective laser signal, and a Polytech PDV-100 laser vibrometer is aimed at the reflective spot. Because the device is operating under electrostatic forces, the frequency that the device outputs will be twice the frequency and half the amplitude of an AC voltage input centered around 0V. A custom testing signal was generated (shown in Fig. 4d) to linearly scale the voltage while avoiding any possible differences between negative and positive charging of the Kapton film. The output from the laser vibrometer was then processed to extract the peaks of the resulting displacement and reconstruct a plot of voltage vs. displacement for 26Hz and 260Hz, also shown in Fig. 4a.

Fig. 4a shows the zero-load displacement results for the transducer. The 26Hz signal clearly shows the threshold voltage effect for the transducer, with voltages below ~550V exhibiting zero displacement and all voltages above ~600V exhibiting around the same displacement, at 0.5mm. The 26Hz signal also behaves similarly to the simulated 0Hz voltage-displacement curves in Fig. 3b. This behavior was expected to be significantly different when the load of the skin is applied, but the asymptotic displacements recorded at the two frequencies will allow us to estimate the approximate difference in displacement between two signals at the same voltage but different frequencies. At 1000V, the 260Hz signal was approximately 8dB lower than the 26Hz signal in terms of displacement. To compare the proximal stimuli (displacement felt at the skin) between the 26Hz and 260Hz signal, we normalized the data so that 0dB corresponded to the 26Hz signal at 100 volume gain and 1000V, while -8dB corresponded to the 260Hz signal at 100 volume and 1000V. While this normalization obscures some of the particulars of the loaded voltage-displacement curves of the device, it allows us to make a direct comparison of perception data between the two frequencies tested.

IV. PSYCHOPHYSICAL EVALUATION

A psychophysical experiment was conducted to estimate the human detection thresholds at two representative frequencies: low (26 Hz) and high (260 Hz). We then estimated the intensity range that can be achieved with the current FET design.

A. Methods

1) Participants

Ten participants (5 females, age 21-27 years old) took part in the study. None of the participants suffered from any sensorimotor deficiency. The participants gave informed consent and were compensated for their time. The study was approved by Dartmouth College's Institutional Review Board (IRB).

2) Apparatus

The experimental apparatus consisted of a FET worn on the dorsal or volar side of either the right or left forearm, in the manner of Fig. 4c. Each participant was given a nitrile glove with the fingers removed that could be fitted to the forearm. The participants could choose whether to place the device on their right or left forearm according to which was more comfortable. The participant rested the chosen arm on a table and held their other arm at their side. The glove was placed on the skin such that it was just beginning to compress the skin, as reported by the participants. The glove acted as a protective insulator in the unlikely event that the Kapton film within the transducer failed. The transducer was attached to the glove with a piece of Scotch tape such that it was slightly pressed into the glove surface. Specifically, the transducer was oriented such that the rigid film was away from the glove and the buckled film was pressing into the glove. In this configuration, the resting state of the buckled film is to be depressed into the skin. When voltage is applied, the buckled film is pulled away from the skin towards the rigid film, breaking contact or decreasing the force. This configuration allows perceivable vibration to be delivered even when the transducer is placed on curved skin or when it is pressed tightly to the skin. The FET was connected by two small wires to the high voltage amplifier, which was connected to the 3.5mm audio jack of a Windows computer through a custom op-amp amplification circuit. Our software consisted of a custom-built MATLAB application that sent out driving signals for the FET as audio signals through the 3.5mm jack. The experimenter used this software to send driving signals to the FET on the participant, and to monitor the signals. The participants wore headphones playing white noise to block audible vibration from the FET throughout the experiment.

3) Procedure

The perceptibility and comfort of the FET were studied in a human detection threshold experiment and a comfort threshold trial. The detection thresholds were estimated at two frequencies, 26 and 260Hz. We employed a three-alternative, one-up three-down adaptive forced-choice procedure [30]. The estimated thresholds correspond to the 79.4 percentile point on a psychometric function [31]. Each of the four tests began with a 0.5 second -4dB signal at a computer volume of 50 (range 0 to 100). This volume was adjusted until the vibration was barely felt, and this was set as the system gain. During each trial, the participant felt three stimuli: two of the stimuli contained no vibration and the remaining contained a vibration. The participant's task was to indicate which interval ("1," "2," or "3") contained the vibration. The vibration magnitude was initially high enough to make sure that the participant understood the task. It was reduced after three consecutive correct responses and increased after one incorrect response. The vibration amplitude was initially changed by 1.5dB for faster convergence and then by 0.5dB after the first two reversals

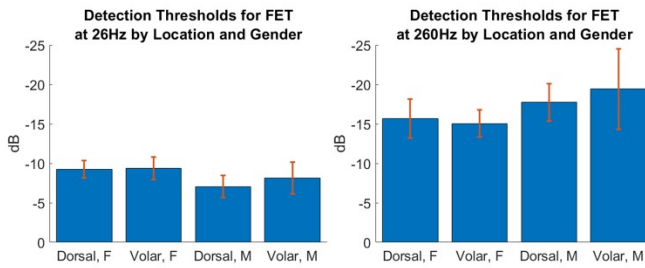


Figure 5: User study. Average detection thresholds at 26Hz (left) and 260Hz (right) from user study. Error bars indicate standard deviations.

for better resolution. A reversal occurred when the amplitude changed from increasing to decreasing, or vice versa. An experimental run was terminated after 8 reversals at the 0.5dB step size. Each run typically lasted 40 to 80 trials.

We used a within-participant design. Each participant completed four conditions: 2 frequencies (26 and 260Hz) and 2 locations (the dorsal and volar sides of the forearm). The condition order was changed between participants. The entire experiment took about 30 minutes per participant. After each condition, the participants were given vibrations of increasing intensity and asked to indicate when the vibrations became uncomfortable or unpleasant. If the vibrations reached the maximum amplitude without becoming uncomfortable, they were recorded as not having felt unpleasant at any vibration. About half the participants found the 260Hz signal uncomfortable at the maximum amplitude, while no one found the 26Hz signal uncomfortable. During certain low-amplitude trials, the subject would become temporarily desensitized to the vibration signal. In these cases, the subject was asked to pause until sensation returned.

4) Data Analysis

Detection threshold was estimated by averaging the peak and valley vibration amplitudes at the last 8 reversals. To estimate the standard deviation of the threshold, four estimates of the threshold were calculated from the four pairs of the peaks and valleys at the 8 reversals, and the corresponding standard deviation was obtained.

B. Results

The average detection thresholds are summarized in Fig. 5. The 26Hz signal had a detection threshold of -8.1dB with a standard deviation of 2.6dB, while the 260Hz signal had a threshold of -17dB and a deviation of 3.4dB. To better understand the effect of factors on the detection thresholds, an ANOVA was conducted with gender, forearm location, and frequency. Neither gender ($p = 0.39$) nor location ($p = 0.52$) was found to be statistically significant. As is apparent in Fig. 5, frequency has a large and significant effect on perception at a given displacement ($p = 0.00$).

The dynamic range of a transducer is an important measure to determine how effectively a transducer can deliver signals. Measured as the difference in dB between the detection threshold and the maximum driving signal, the dynamic range for both signals was found to be around 10dB, though higher ranges should be achievable with higher voltages and different geometries. A taller airgap leads to greater maximum displacement, higher threshold voltage, and sharper threshold transition.

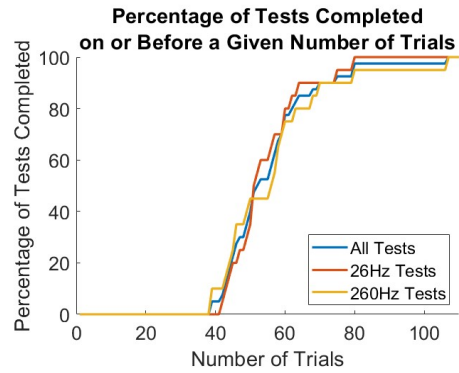


Figure 6: Percentage of tests completed on or before a given number of trials. Trials were counted starting from the first reversal.

V. GENERAL DISCUSSION

We hypothesize that the lack of differentiation between genders or locations is mostly a result of the device’s displacement-voltage curve. Displacement does not smoothly increase with signal strength, but rather rapidly switches from a “mostly off” to “mostly on” state. The precise strength at which this switch occurs changes between participants, based on their physiological parameters and device placement. The perceived vibration is dominated by whether the signal strength is above or below this switching threshold. We believe that this insensitivity to gender and location could make the transducer well-suited to haptic wearables, as it eliminates the need for extensive calibration.

To better understand the rate at which the transducer moved from “mostly off” to “mostly on”, we examined the time it took for the participant to complete the trial as a proxy. If the transducer were binary, then participants would rapidly find their detection threshold (as the delivered signal strength would oscillate between a value at which the transducer had no response and a slightly larger value at which it had a strong response). If the transducer had a linear response, this would result in longer trials (as the delivered signal strength would often be near the detection threshold).

Fig. 6 plots the percentage of tests completed on or before a certain number of trials. All participants were able to complete all tests in under 110 trials. Approximately half the tests were completed with under 60 trials, which indicates a relatively steep displacement-signal strength relationship at the switching voltage. We examined whether gender, frequency, or location had any effect on the participant speed. According to a set of T-tests, none of the three variables had any statistically significant effect on the number of trials needed. The p-values for location, gender, and frequency were 0.80, 0.84, and 0.42 respectively. The lack of dependence on these variables indicates the usability of the transducer in real-world applications. Based on the zero-load voltage-displacement curves in Fig. 4a, we would expect the tests at 26Hz to be completed more quickly than those at 260Hz, but this was not the case. We hypothesize that there is a broadening of the threshold driving signal that occurs when the transducer is pressed to the skin as opposed to open to the air. This would serve to modify the 26Hz and 260Hz responses such that they have similar characteristics.

VI. CONCLUSION

A flexible electrostatic transducer was designed, built, and tested as an actuator for haptic communication wearables. The transducer was both simulated and measured experimentally to optimize its geometry and haptics function. We found that the output of the transducer onto the skin was insensitive to gender and forearm location, which indicates that it is well suited for use in a haptic device with little to no calibration. Further planned modifications to the transducer design will allow us to bring down the required voltage of the transducer significantly, which will allow it to be more easily integrated into a compact wearable. Finally, we plan to miniaturize and tessellate the transducer into a haptic matrix to increase transmitted information density.

The estimated dynamic range of 10dB places a lower bound on the ranges of transducers of this design. By increasing the actuator height and changing the film material, it is possible to increase the dynamic range to 30-40dB. The operating voltage scales with the square of the thickness of the rigid film, so cutting the rigid film thickness from 25 μm to 5 μm should cut the operating voltage from 0-1000V to 0-40V. Operating at higher voltages will then allow the dynamic range to be increased. Increasing the transducer height and stiffness can also have positive effects on displacement and dynamic range. Modifications to the existing designs, including adding bistability, have the potential to further increase the intensity range. With these improvements, the FET could be used in applications outside of haptics, including as flexible speakers, high-precision displacement actuators, or capacitive sensors.

REFERENCES

- [1] C. M. Reed, N. I. Durlach, and L. A. Delhorne, "Natural Methods of Tactile Communication," in *Tactile Aids for the Hearing Impaired*, I. R. Summers, Ed. London: Whurr Publishers, 1992, pp. 218–230.
- [2] S. D. Novich and D. M. Eagleman, "Using space and time to encode vibrotactile information: toward an estimate of the skin's achievable throughput," *Exp. Brain Res.*, vol. 233, no. 10, pp. 2777–2788, 2015.
- [3] G. Luzhnica, E. Veas, and V. Pammer, "Skin Reading: Encoding Text in a 6-Channel Haptic Display," *Proc. 2016 ACM Int. Symp. Wearable Comput.*, pp. 148–155, 2016.
- [4] S. Zhao, A. Israr, F. Lau, and F. Abnoui, "Coding Tactile Symbols for Phonemic Communication," *Proc. 2018 CHI Conf. Hum. Factors Comput. Syst. - CHI '18*, p. 392, 2018.
- [5] R. Turcott *et al.*, "Efficient Evaluation of Coding Strategies for Transcutaneous Language Communication," in *International Conference on Human Haptic Sensing and Touch Enabled Computer Applications*, 2018, pp. 600–611.
- [6] H. Z. Tan, N. I. Durlach, C. M. Reed, and W. M. Rabinowitz, "Information Transmission with a Multifinger Tactile Display," *Percept. Psychophys.*, vol. 61, no. 6, pp. 993–1008, 1999.
- [7] H. Z. Tan, C. M. Reed, and N. I. Durlach, "Optimum Information Transfer Rates for Communication through Haptic and Other Sensory Modalities," *IEEE Trans. Haptics*, vol. 3, no. 2, pp. 98–108, 2010.
- [8] A. Haans and W. IJsselstein, "Mediated Social Touch: A Review of Current Research and Future Directions," *Virtual Real.*, vol. 9, no. 2–3, pp. 149–159, 2006.
- [9] K. Kim, X. Ren, S. Choi, and H. Z. Tan, "Assisting People with Visual Impairments in Aiming at a Target on a Large Wall-Mounted Display," *Int. J. Hum. Comput. Stud.*, vol. 86, pp. 109–120, 2016.
- [10] J. Park, Y. Oh, and H. Z. Tan, "Effect of Cutaneous Feedback on the Perceived Hardness of a Virtual Object," *IEEE Trans. Haptics*, vol. 11, no. 4, pp. 518–530, 2018.
- [11] J. Park, W. R. Provancher, and H. Z. Tan, "Haptic Perception of Edge Sharpness in Real and Virtual Environments," *IEEE Trans. Haptics*, vol. 10, no. 1, pp. 54–62, 2017.
- [12] C. M. Reed *et al.*, "A Phonemic-Based Tactile Display for Speech Communication," *IEEE Trans. Haptics*, vol. 12, no. 1, pp. 2–17, 2019.
- [13] N. Dunkelberger *et al.*, "Conveying Language through Haptics: A Multi-sensory Approach," in *Proceedings of the 2018 ACM International Symposium on Wearable Computers*, 2018, pp. 25–32.
- [14] L. Dong *et al.*, "Flexible Porous Piezoelectric Cantilever on a Pacemaker Lead for Compact Energy Harvesting," *Adv. Mater. Technol.*, vol. in press, pp. 1–9, 2019.
- [15] D. Chen, K. Chen, K. Brown, A. Hang, and J. X. J. Zhang, "Liquid-phase tuning of porous PVDF-TrFE film on flexible substrate for energy harvesting for energy harvesting," *Appl. Phys. Lett.*, vol. 110, no. 15, p. 153902, 2017.
- [16] N. Hu *et al.*, "Edge effect of strained bilayer nanofilms for tunable multistability and actuation," *Nanoscale*, vol. 9, pp. 2958–2962, 2017.
- [17] D. Chen, C. Wang, W. Chen, Y. Chen, and J. X. J. Zhang, "PVDF-Nafion nanomembranes coated microneedles for in vivo transcutaneous implantable glucose sensing," *Biosens. Bioelectron.*, vol. 74, pp. 1047–1052, 2015.
- [18] T. Sharma, S. Naik, J. Langevine, B. Gill, and J. X. J. Zhang, "Aligned PVDF-TrFE Nanofibers With High-Density PVDF Nanofibers and PVDF Core-Shell Structures for Endovascular Pressure Sensing," *IEEE Trans. Biomed. Eng.*, vol. 62, no. 1, pp. 188–195, Jan. 2015.
- [19] R. Legtenberg, J. Gilbert, S. D. Senturia, and M. Elwenspoek, "Electrostatic Curved Electrode Actuators," *J. Microelectromechanical Syst.*, vol. 6, no. 3, pp. 257–265, 1997.
- [20] R. Jebens, W. Trimmer, and J. Walker, "Microactuators for Aligning Optical Fibers," *Sensors and Actuators*, vol. 20, no. 1–2, pp. 65–73, 1989.
- [21] S. Rosset and H. R. Shea, "Flexible and stretchable electrodes for dielectric elastomer actuators," *Appl. Phys. A Mater. Sci. Process.*, vol. 110, no. 2, pp. 281–307, 2013.
- [22] A. Marette, A. Poulin, N. Besse, S. Rosset, D. Briand, and H. Shea, "Flexible Zinc-Tin Oxide Thin Film Transistors Operating at 1 kV for Integrated Switching of Dielectric Elastomer Actuators Arrays," *Adv. Mater.*, vol. 29, no. 30, pp. 1–6, 2017.
- [23] M. Mohiuddin, H. U. Ko, H. C. Kim, J. Kim, and S. Y. Kim, "Transparent and flexible haptic actuator based on cellulose acetate stacked membranes," *Int. J. Precis. Eng. Manuf.*, vol. 16, no. 7, pp. 1479–1485, 2015.
- [24] S. J. Bolanowski, G. A. Gescheider, R. T. Verrillo, and C. M. Checkosky, "Four Channels Mediate the Mechanical Aspects of Touch," *J. Acoust. Soc. Am.*, vol. 84, no. 5, pp. 1680–1694, 1988.
- [25] R. T. Verrillo and G. A. Gescheider, "Perception via the Sense of Touch," in *Tactile Aids for the Hearing Impaired*, S. I., Ed. London: Whurr Publishers, 1992, pp. 1–36.
- [26] I. Trase *et al.*, "Low Power Flexible Electrostatic Transducers for Haptic Communication," in *Materials Research Society Fall Meeting*, 2018.
- [27] K. A. Kaczmarek, J. G. Webster, P. Bach-y-Rita, and W. J. Tompkins, "Electrotactile and Vibrotactile Displays for Sensory Substitution Systems," *IEEE Trans. Biomed. Eng.*, vol. 38, no. 1, pp. 1–16, 1991.
- [28] C. Makous, M. Friedman, and J. Vierck, "A Critical Band Filter in Touch," *J. Neurosci.*, vol. 15, no. 4, pp. 2808–2818, 1995.
- [29] W. H. Talbot, I. Darian-Smith, H. H. Kornhuber, and V. B. Mountcastle, "The Sense of Flutter-Vibration: Comparison of the Human Capacity with Response Patterns of Mechanoreceptive Afferents from the Monkey Hand," *J. Neurophysiol.*, vol. 31, no. 2, pp. 301–334, 1968.
- [30] L. A. Jones and H. Z. Tan, "Application of Psychophysical Techniques to Haptic Research," *IEEE Trans. Haptics*, vol. 6, no. 3, pp. 268–284, 2013.
- [31] H. Levitt, "Transformed Up-Down Methods in Psychoacoustics," *J. Acoust. Soc. Am.*, vol. 49, no. 2B, pp. 467–477, 1971.